Procedia
Environmental Science, Engineering and Management
http://www.procedia-esem.eu

Procedia Environmental Science, Engineering and Management **8** (2021) (1) 205-214

Environmental Innovations: Advances in Engineering, Technology and Management, EIAETM, 19th-23rd October, 2020

TESTING OF A RESISTIVE SENSOR WITH FABRIC MEDIUM FOR MONITORING FROST FORMATION IN REFRIGERATION SYSTEMS*

Martim L. Aguiar[1,2], Pedro D. Gaspar[1,2,], Pedro D. Silva[1,2], Diana Duarte[3]**

[1]University of Beira Interior, Covilhã, Portugal
[2]C-MAST - Centre for Mechanical and Aerospace Science and Technologies, Covilhã, Portugal
[3]ITJ Moldes, Marinha Grande, 2431-966, Portugal

Abstract

Refrigeration is one of the key elements for food preservation. With global temperatures increasing due to global warming, the efficiency in refrigerated storage systems must be improved. One of the problems that is yet to be solved in these systems is the efficient and accurate removal of the frost formed on the heat exchanger surface. In previous works, a low-cost resistive sensor has been developed to detect frost formation for accurate removal. This paper shows the results of an experimental study carried out to increase the accuracy, by placing different configurations of a fabric medium in between the sensor electrodes.

Keywords: defrosting, evaporators, frost, refrigeration, sensor

1. Introduction

Frost formation on the fin-and-tube evaporators has been widely studied, and yet it is one of the main causes of inefficiency. The fin-and-tube evaporators used in light commercial systems have a large area-to-volume ratio. The demand for subfreezing operating temperatures causes the formation of a frost layer on the fin surface as shown on Fig. 1.

A frost layer is a porous medium comprised of ice crystals and pores filled with moist air. The frost build-up on the evaporators fin surface increases its air-side thermal resistance, decreasing the overall efficiency of the system. This frost accumulation may, in extreme cases, lead to the blockage of the air passage between the fins.

* Selection and peer-review under responsibility of the EIAETM
** Corresponding author: e-mail: martim.aguiar@ubi.pt; dinis@ubi.pt

Full blockage of the evaporator can occur if no defrost method is applied. Several parameters can influence frost growth, but those with most influence are air relative humidity, velocity and supercooling degree (Panoias et al., 2019), but may also be influenced by other parameters such as fin shape and spacing, type of flow, or air cleanliness. The lower system efficiency caused by the frost layer on fin surfaces results in a higher energy demand, and in extreme cases, system damage, and may even result in a threat to food safety (Hermes et al., 2009). Defrost methods are used to reduce the problem, although additional energy is usually also consumed for them to operate (Wang et al., 2018). These defrost methods can be classified as seen in Fig. 2.

Time controlled with on-off defrosting and electric resistive heater or reverse cycle are still one of the most used defrosting methods. Apart from these, none of the abovementioned methods has gained significant acceptance from the refrigeration industry, due to complex, expensive, and unreliable sensing and prediction methods (Xiao et al., 2010). This can cause a huge impact on energy consumption, as the timed defrost operations have to be scheduled for the worst-case scenario (warm air with high relative humidity) and thus, as these properties vary during the year, the amount of defrosting cycles could vary as well. (Tassou et al., 2001) studied frost formation and defrost control parameters for vertical open refrigerated display cabinets (VORDC) and concluded that the ideal time between defrosts varies greatly with air temperature and humidity.

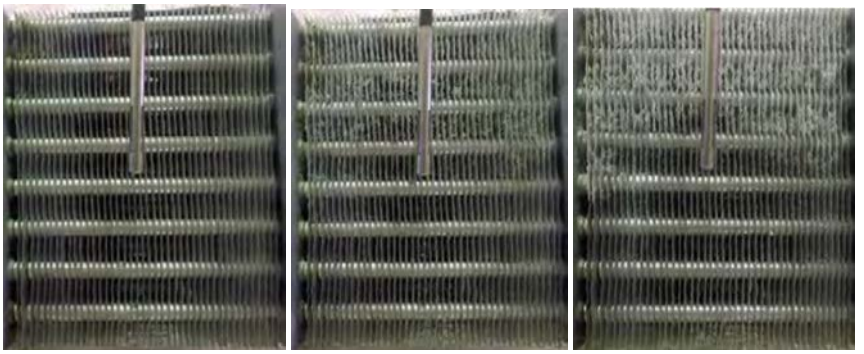

Fig. 1. Different amounts of frost accumulated on heat exchanger fins (Panoias et al., 2019).

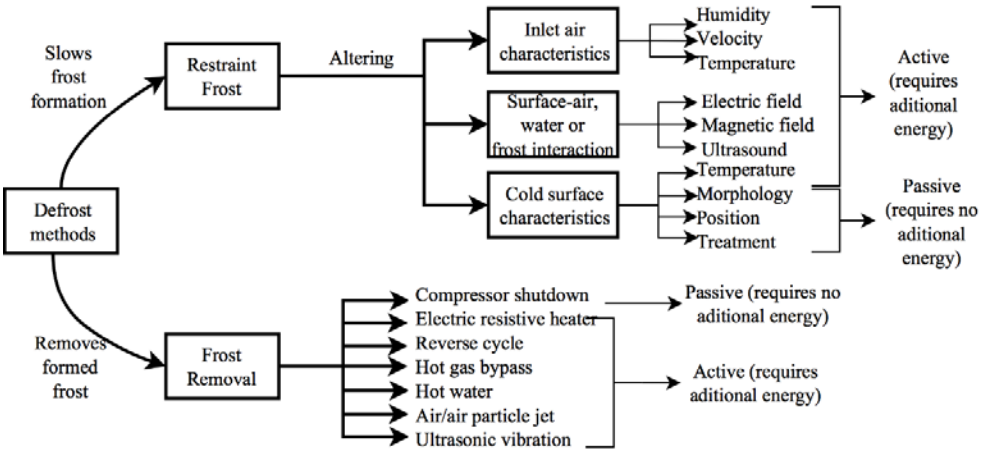

Fig. 2. Classification of available defrost methods (De Aguiar et al., 2019).

As shown in Fig. 3, the ideal operation time between defrosts on VORDC can range from 4 hours to around 9.5 hours during different times of the year, according to the variation of the parameters that affect frost growth.

Demand defrost tries to solve this problem by measuring or predicting frost formation. This prediction can be achieved by computing the measured factors that influence frost formation – such as heat exchanger surface temperature, and inlet air characteristics: relative humidity, temperature and velocity; computing the measurable system changes caused by the frost accumulation on the evaporator – temperature difference between the air and evaporator surface, pressure drop, degree of refrigerant superheat, fan power sensing; or both, using methods such as artificial intelligence and other algorithms. Alternatively, demand defrost cycles can be controlled by directly measuring frost on the evaporator coils. In this scenario no prediction is necessary, as sensors positioned on the evaporator directly evaluates the state of the frost accumulation and their data is processed so that the defrost operation occurs when best suited (De Aguiar et al., 2019).

The electrical resistance of a given sample varies with its shape and material. Air, ice and water have quite different electrical resistance values, meaning that if two electrodes are positioned in the evaporator (but close enough for a voltage drop to be measured) and a voltage is applied on the terminals, a characteristic voltage drop will be measured as water forms, and this voltage drop will increase as this water freezes, indicating ice formation. A device based on this characteristic was developed by (Graça et al., 2016) and (Caetano et al., 2018). The principle of the sensor is based on the equation 1:

$$R = \rho \cdot L/A \tag{1}$$

Where R [Ω] is the measured resistance, ρ [Ω·m] the resistivity of the material between the electrodes which is the variable that has different values for water, ice or air, L [m] the length of this material (directly related with the distance between the electrodes), and A [m^2] the section area of this material. If the electrodes are close enough, a bridge between the electrodes is formed, as seen on Fig. 4. This condensed water will result in a decrease of the resistance between the sensor terminals.

In (De Aguiar et al., 2020), different resistive sensors with variable electrode configurations were tested, and promising results were obtained. The most promising results were obtained with the sensor shown in Fig. 5.

This sensor has two different electrodes. The first electrode acts as a clamp to fix the sensor on a fin of the heat exchanger, allowing for a lower thermal resistance between the sensor and fin surfaces, ensuring frost formation on the sensor. The second electrode is a wire with a diameter of 0.5 mm and a length of 6 mm, parallel to the first electrode, and facing the air intake vertically. The electrodes are separated by an air gap of approximately 0.6 mm. This sensor was able to detect 3 out of 5 frost-defrost cycles, as shown in Fig. 6.

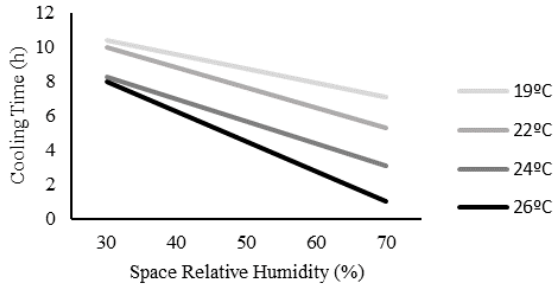

Fig. 3. Optimum time between defrosts – adapted from (Tassou et al., 2001).

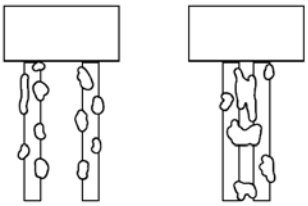

Fig. 4. Water droplets (left) and bridges (right) on the electrodes (De Aguiar et al., 2019).

Fig. 5. CAD model (left) and picture (right) of the sensor with the best results (De Aguiar et al., 2020).

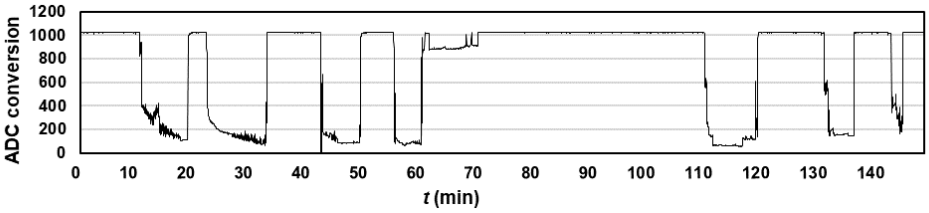

Fig. 6. Results obtained with the resistive sensor (De Aguiar et al., 2020).

A sensor to be implemented for frost detection has to be reliable, in order to avoid malfunctioning of the refrigeration systems, so the possibilities that may have resulted in failure on previous studies (such as the failure in the detection of the third cycle on Fig. 6.) have to be tackled. Some of the problems detected are the precipitation of the droplet that connects the sensor electrodes with vibrations, and the accidental touching between sensor electrodes, and/or sensor electrodes and a heat exchanger surface that is not electrically insulated. Both these problems can be solved by insulating the terminals with a material that is not electrically conductive and permeable to water. This way, the smallest amount of water is transported between the electrodes, creating a humid medium that becomes electrically conductive, and does not precipitate with vibrations. This also maintains the distance between electrodes constant and allows contact between the sensor and heat exchanger surface without fears of causing interference.

For the present work, cotton string, and cotton sewing thread were tested as a medium, in different sensors with different configurations.

2. Experimental Setup

An analog-to-digital converter (ADC) uses a voltage divider to measure the voltage drop between the electrodes as shown in Fig. 7. The ADC returns a value between 0 and 1023, that represents lower and higher resistances, respectively. Ice and air should be expected to give values near 1023, as they have high resistive values, and water should have

a lower value, if a water bridge forms between the electrodes, or in this case, the humidity in the cotton string increases.

Different cotton strings and electrode configurations were tried to form a water bridge and allow the sensor to detect water accumulation before frosting. Five different copper electrode sensors were tested, in different configurations:

2.1. Sensor 1

The sensor 1 is made from two cylindrical parallel copper electrodes with a diameter of 0.5 mm, separated by a cotton sewing thread, tightly tied in a form of ∞ around both electrodes. This sensor is positioned on the refrigerant tube, between fins, facing the intake front of the evaporator. The sensor model (left) and tested sensor (right) are shown in Fig. 8.

2.2. Sensor 2:

The sensor 2 is a variation of the sensor 1, that instead of embracing the refrigerant tube, embraces the fin, it is also made from two cylindrical parallel copper electrodes with a diameter of 0.5 mm, separated by a cotton sewing thread, tied in a form of ∞ around both electrodes. This sensor is longer to clamp the fin. The sensor model (left) and tested sensor (right) are shown in Fig. 9.

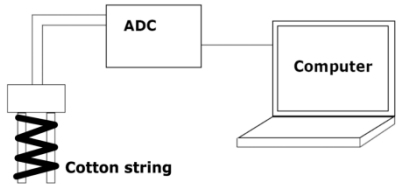

Fig. 7. Experimental setup scheme – adapted from (De Aguiar et al., 2019).

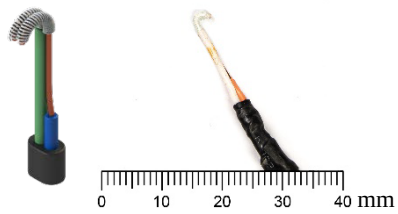

Fig. 8. CAD model (left) and picture (right) of the sensor 1.

Fig. 9. CAD model (left) and picture (right) of the sensor 2.

2.3. Sensor 3:

The sensor 3 is made from two parallel rectangular copper electrodes separated by a cotton string (thicker than the cotton sewing thread), tied in a form of ∞ around both electrodes, each with a dimension of 0.6×1.1×12 mm^3. One of the electrodes has a plate that can be wedged between fins so that the sensor electrodes can be parallel to the heat exchanger front and faces the intake air. Because of the wedged plate, heat can be more efficiently conduced and therefore bring down the electrode temperature. This sensor has a higher contact area with the intake air. The sensor model (left) and tested sensor (right) are shown in Fig. 10.

2.4. Sensor 4:

The sensor 4 is very similar to sensor 2, with the only difference being that it uses cotton string loosely tied, instead of tightly tied cotton sewing thread. The sensor model (left) and tested sensor (right) are shown in Fig. 11.

2.5. Sensor 5:

The sensor 5 has four electrodes, connected alternately to two terminals. It is as if two sensors like the sensor 2 were glued and connected to the same cables. The sensor embraces the fin and faces the intake front of the heat exchanger. It is made from four cylindrical parallel copper electrodes with a diameter of 0.5 mm, separated by a cotton sewing thread, tightly tied in a form of around both electrodes. This sensor is wider to increase the surface that gets in contact with the air, and to smooth the curve obtained by the ADC data. The sensor model (left) and tested sensor (right) are shown in Fig. 12.

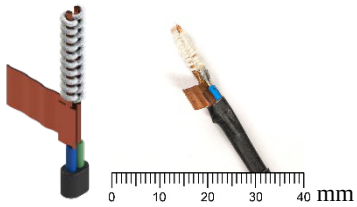

Fig. 10. CAD model (left) and picture (right) of the sensor 3.

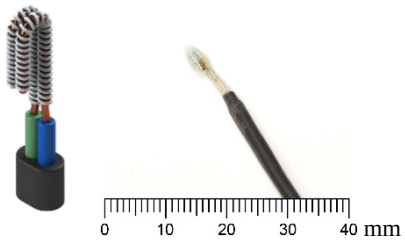

Fig. 11. CAD model (left) and picture (right) of the sensor 4.

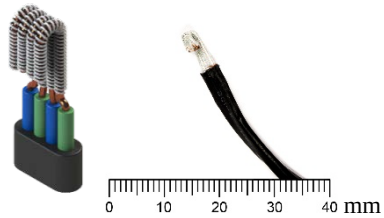

Fig. 12. CAD model (left) and picture (right) of the sensor 5.

3. Results

3.1. Sensor 1

Sensor 1 was placed on the refrigerant tube, between fins, and at first glance, it appears that it failed to detect the water deposition and frost on the sensor, although it clearly detected the defrosts. On Fig. 13 on the left the results of a test can be seen, in which two frost-defrost cycles were made, the first defrost started at t = 20 min and the second at t = 69 min.

On the right, the ADC conversion axis values are cropped between 950 and 1050 so that the fluctuations are more visible, and it can be seen that water deposition is detected in $t \in$ [20, 23[min and $t \in$ [20, 23[min.

3.2. Sensor 2

The sensor 2 had worse results than the sensor 1. A tighter wrap of the cotton string made it so that the electrodes were so insulated that no water was deposited in between them. Fig. 14. shows the results of a single frost-defrost cycle. On the left we can see that even during the defrost, the sensibility of this sensor is reduced. On the right, with the ADC conversion axis amplified, it is possible to confirm the detection of a defrost cycle that started at t = 14 min.

3.3. Sensor 3

The sensor 3 did not yield good results either, as shown in Fig. 15 on the left. With amplification of the ADC conversion axis the measurement fluctuations are more visible, with a lot of noise. Two frost-defrost cycles were done, and only the defrosts (started at t = 17 min and t = 60 min) were detected, although with very low sensitivity as shown on Fig. 15 on the right.

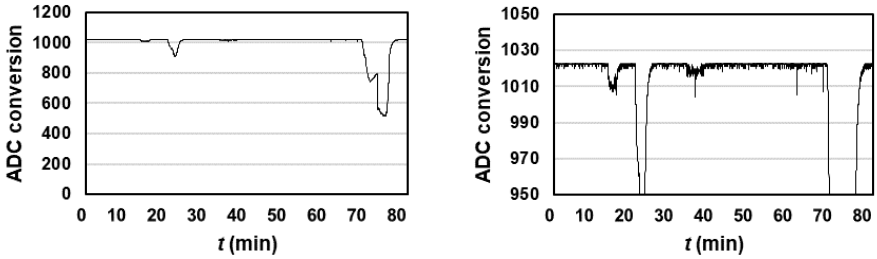

Fig. 13. Results for the sensor 1.

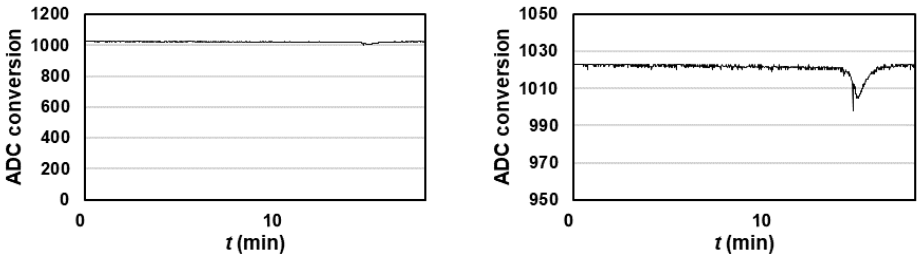

Fig. 14. Results for the sensor 2.

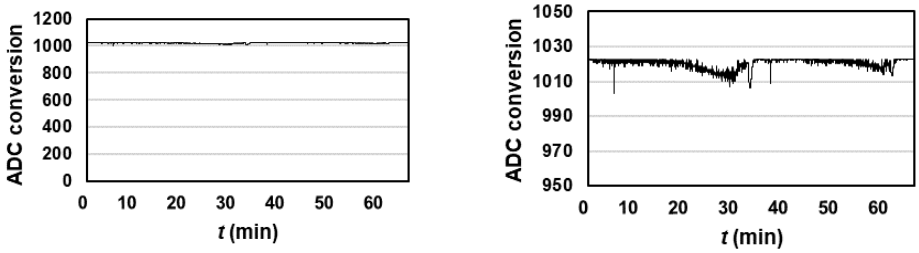

Fig. 15. Results for the sensor 3.

3.4. Sensor 4

Sensor 4 was the most promising, detecting all the frost-defrost cycles in 5 consecutive cycles. This is shown in Fig. 16. with no need to amplify the ADC conversion axis, with water accumulation during the frost phase of the cycle being detected in $t \in [1, 21[$ min; $t \in [45, 70[$ min; $t \in [91, 117[$ min; $t \in [153, 174[$ min and $t \in [207, 219[$ min and defrosts that started at t = 33 min, t = 75 min, t = 135 min, t = 186 min, and t = 229 min. Another interesting observation is the difference between the curves on the frosting and defrosting parts of the cycle, being the frosting curves the most irregular and the defrosting curves a lot smoother.

3.5. Sensor 5

The sensor 5 was not as effective as sensor 4, the sensitivity is lower, but the curves are smoother as shown in Fig. 17.

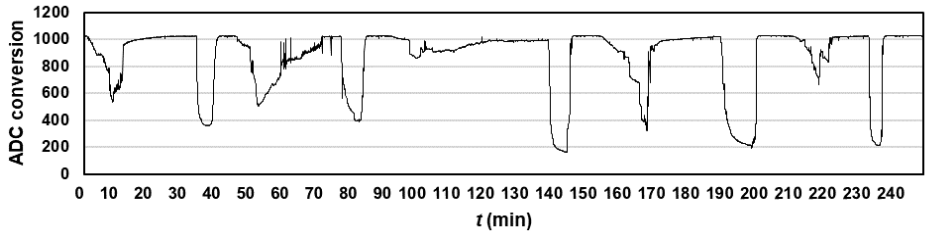

Fig. 16. Results for the sensor 4.

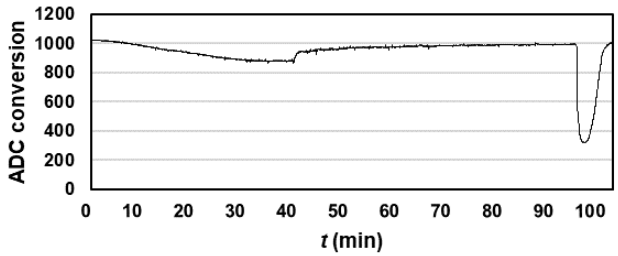

Fig. 17. Results for the sensor 5.

Most likely due to the increase in the number of sensor terminals. The detection of water between electrodes on the interval $t \in [2, 86[$ min is especially long mainly for two reasons: first, the increased amount of terminals increases the surface area, and more water that has to be completely frozen in order to get the ADC conversion value back to 1023, and second, the fin in which the sensor was placed took an especially long time to completely freeze as it was in a spot of the heat exchanger that took longer to freeze.

4. Conclusions

It is possible to detect frost formation and defrosting operations using a low-cost resistive sensor, and although a perfectly accurate and reliable version has not yet been achieved. Adding an absorbent material between the sensor electrodes might be a solution to increase the reliability of a resistive sensor. Fig. 6. shows the best result achieved without the use of an absorbent material between electrodes, where three out of four frost-defrost cycles are detected. This result has now been improved by achieving five out of five frost-defrost cycles with sensor 4, as seen in Fig. 14.

If a resistive sensor does not distinguish between air and ice, it is possible to determine the values that the sensor is reading as there is no transition from ice to air or vice versa without passing through a water phase, and therefore, if a reliable enough sensor is developed, it might be a viable and low-cost solution for industrial application.

When comparing the curves in Fig. 14. and Fig. 6., the results of consecutive frost-defrosting operations, result in quite different curve shapes. The defrosting operation curve is smoother for the sensor with cotton fabric between electrodes, and it is easy to distinguish between frosting and defrosting by the shape of the curve, which might be useful for the implementation in a refrigeration system.

Even though it was possible to detect 5 frost-defrost operations, sensor 4 still gives an irregular signal that has a lot of noise while detecting the frost formation. Adifferent medium or increasing the number of sensor electrodes might result in a more uniform signal across the cycles.

Sensors 1, 2 and 5 have low sensitivity, suggesting that tightly tied sensors sacrifice sensibility for toughness, which might not be a desirable trade. The usage of cotton as the medium between the electrodes has the disadvantage of thermally insulating the sensor terminals, making it harder to reach dew point on the surface of the sensor, resulting in less water deposited during frosting. This might be one of the reasons why sensors with tightly tied cotton sewing thread have worse results.

The use of material that is absorbent, electrical insulator, but also a good heat conductor (such as some ceramics) might be an improvement from the current use of a fabric as medium.

Having a material between electrodes also ensures that vibrations do not cause the water to precipitate, while assuring an even and constant distance between electrodes, and

electrical insulation from the heat exchanger. The sensor size is still an advantage, as sensors with a few millimeters are already able to detect frost formation with more reliability than larger sizes from previous studies. This small size decreases the disturbance in the air flow on the heat exchanger. Additional studies are being conducted to evaluate the characteristics and performance of such materials for frost detection purposes.

A reliable sensor for the detection of frost formation in evaporators might be a simple, yet effective way to reduce energy consumption on refrigeration systems, but further studies should be done to achieve higher reliability.

Acknowledgements

This study is within the activities of project "Pack2Life – High performance packaging", project IDT in consortium No.33792, call No.03/SI/2017, Ref. POCI-01-0247-FEDER-033792, promoted by COMPETE 2020 and co-funded by FEDER within Portugal 2020.

This work has been supported by the project Centro-01-0145-FEDER000017 - EMaDeS - Energy, Materials and Sustainable Development, co-funded by the Portugal 2020 Program (PT 2020), within the Regional Operational Program of the Center (CENTRO 2020) and the European Union through the European Regional Development Fund (ERDF).

The authors thank the opportunity and financial support to carry on this project to Fundação para a Ciência e Tecnologia (FCT) and R&D Unit "Centre for Mechanical and Aerospace Science and Technologies" (C-MAST), under project UIDB/00151/2020.

References

Caetano D., Gaspar P.D., Da Silva P.D., (2018), Experimental testing of a resistive sensor for monitoring frost formation in refrigeration systems, In *CYTEF 2018 - IX Congreso Ibérico y VII Congreso Iberoamericano de Ciencias y Técnicas del Frío Proceedings*, International Institute of Refrigeration, Valencia, Spain, 6.

De Aguiar M.L., Gaspar P.D., Da Silva P.D., (2019), Further development and experimental testing of a resistive sensor for monitoring frost formation in refrigeration systems, In *ICR 2019 refrigeration science and technology proceedings*, International Institute of Refrigeration, Montreal, Quebec, Canada, 2191-2200.

De Aguiar M.L., Gaspar P.D., Da Silva P.D., (2020), Optimization and further experimental testing of a resistive sensor for monitoring frost formation in refrigeration systems, International Institute of Refrigeration, Nantes, France, 2191-2200.

Graça M., Gaspar P.D., Silva P.D. da, Nunes J., Andrade L.P., (2016), Monitoring device of ice formation in evaporator surface of refrigeration systems, In *VI Ibero-American Refrigeration Sciences and Technologies*, International Institute of Refrigeration, Coimbra, Portugal, 8, On line at: https://ubibliorum.ubi.pt/handle/10400.6/7363?mode=full.

Hermes C.J.L., Piucco R.O., Barbosa J.R., Melo C., (2009), A study of frost growth and densification on flat surfaces, *Experimental Thermal and Fluid Science*, **33**, 371-379.

Panoias P., Silva P.D., Pires L.C., Gaspar P.D., Nunes J., (2019), Experimental tests using deactivation of coolant fluid circulation to mitigate frost formation on the heat exchanger surface, In *ICR 2019 refrigeration science and technology proceedings*, International Institute of Refrigeration, Montreal, Quebec, Canada, 2424-2430.

Tassou S.A., Datta D., Marriott D., (2001), Frost formation and defrost control parameters for open multideck refrigerated food display cabinets, *Proceedings of the Institution of Mechanical Engineers, Part A: Journal of Power and Energy*, **215**, 213-222.

Wang F., Liang C., Zhang X., (2018), Research of anti-frosting technology in refrigeration and air conditioning fields: A review, (in en), *Renewable and Sustainable Energy Reviews*, **81**, 707-722.

Xiao J., Wang W., Guo Q.C., Zhao Y.H., (2010), An experimental study of the correlation for predicting the frost height in applying the photoelectric technology, *International Journal of Refrigeration*, **33**, 1006-1014.